

# SnI<sub>4</sub><sup>2-</sup>-Based Hybrid Perovskites Templated by Multiple Organic Cations: Combining Organic Functionalities through Noncovalent Interactions

Zhengtao Xu and David B. Mitzi\*

IBM T. J. Watson Research Center, P.O. Box 218, Yorktown Heights, New York 10598

Received April 15, 2003. Revised Manuscript Received June 27, 2003

Two and more different organic cations have been incorporated within single-phase hybrid perovskite frameworks derived from SnI<sub>4</sub><sup>2-</sup> layers. The single-crystal structure of (5FPEA·NEA)SnI<sub>4</sub>, containing in 1:1 ratio the 2,3,4,5,6-pentafluorophenethylammonium (5FPEA) and 2-naphthyleneethylammonium (NEA) cations [*C2/m*, *a* = 37.040(7) Å, *b* = 6.161(1) Å, *c* = 12.345(3) Å, *β* = 101.84(3)°, and *Z* = 4], provides details of the packing and interaction of the two organic species confined within the inorganic sheets. Controlled crystallization from solutions suggests that the 1:1 ratio is thermodynamically favored, perhaps as a result of the fluoroaryl–aryl interaction between the two organic cations. Systems with other ratios of the above two cations, however, can be accessed as thin films by spin coating from organic solutions. Structure and property studies indicate that the ratio of the organic cations is in monotonic correlation with the spacing of the perovskite sheets as well as the exciton energy associated with the electronic band gap. This study provides a simple method of modifying the electronic properties and combining organic functionalities within hybrid perovskites—a method that is based on noncovalent interactions (i.e., physical combination) instead of the traditional organic synthesis.

## Introduction

Recently, great attention has been directed at a group of hybrid perovskites based on metal halide frameworks and organic cations, partly due to the structural flexibility of the organic as well as the inorganic components.<sup>1–3</sup> In the most commonly studied systems, the inorganic portion consists of perovskite-like layers based on corner-sharing metal halide octahedral units (e.g., SnX<sub>6</sub><sup>2-</sup>, PbX<sub>6</sub><sup>2-</sup>, and CdX<sub>6</sub><sup>2-</sup>), whereas the organic portion is usually an organic ammonium cation, balancing the negative charge from the inorganic layer. Useful properties derived from the inorganic moiety include good electrical mobility,<sup>4–8</sup> band gap tunability,<sup>6–12</sup> mechanical and thermal stability, and interesting magnetic<sup>13–17</sup> or dielectric transitions.<sup>18–20</sup> Meanwhile, the organic moiety offers potential advantages such as

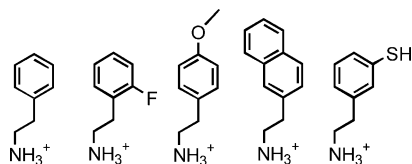
plastic mechanical properties, convenient processing, and the structural and functional diversity typical of organic materials.

Our lab is interested in using the organic functionalities to modify the electronic properties of the semiconductive SnI<sub>4</sub><sup>2-</sup>-based compounds [e.g., (PEA)<sub>2</sub>SnI<sub>4</sub>, PEA: phenethylammonium]. Recently,<sup>21–23</sup> it has been demonstrated that by using steric hindrance and other structural effects from the organic components, one can effectively impact the structure of the inorganic framework and consequently shift the exciton wavelengths associated with the band gap within a wide range from 545 to 630 nm. Substituent groups on the organic cation have also been shown to affect the thermal transition properties of the hybrid perovskite materials.<sup>24,25</sup> Stud-

\* Corresponding author.

- (1) Mitzi, D. B. *Prog. Inorg. Chem.* **1999**, *48*, 1.
- (2) Mitzi, D. B. *J. Chem. Soc., Dalton Trans.* **2001**, 1.
- (3) For early studies on organic–inorganic hybrids, see: (a) Buckley, A. M.; Bramwell, S. T.; Visser, D.; Day, P. *J. Solid State Chem.* **1987**, *69*, 240. (b) Day, P.; Ledsham, R. D. *Mol. Cryst. Liq. Cryst.* **1982**, *86*, 163.
- (4) Kagan, C. R.; Mitzi, D. B.; Dimitrakopoulos, C. D. *Science* **1999**, *286*, 945.
- (5) Mitzi, D. B.; Chondroudis, K.; Kagan, C. R. *IBM J. Res. Dev.* **2001**, *45*, 29.
- (6) Mitzi, D. B.; Feild, C. A.; Harrison, W. T. A.; Guloy, A. M. *Nature* **1994**, *369*, 467.
- (7) Mitzi, D. B.; Wang, S.; Feild, C. A.; Chess, C. A.; Guloy, A. M. *Science* **1995**, *267*, 1473.
- (8) Mitzi, D. B.; Feild, C. A.; Schlesinger, Z.; Laibowitz, R. B. *J. Solid State Chem.* **1995**, *114*, 159.
- (9) Mitzi, D. B. *Chem. Mater.* **1996**, *8*, 791.
- (10) Papavassiliou, G. C.; Koutselas, I. B. *Synth. Met.* **1995**, *71*, 1713.
- (11) Weber, D. Z. *Naturforsch.* **1979**, *34b*, 939.
- (12) Weber, D. Z. *Naturforsch.* **1978**, *33b*, 862.
- (13) De Jongh, L. J.; Botterman, A. C.; De Boer, F. R.; Miedema, A. R. *J. Appl. Phys.* **1969**, *40*, 1363.
- (14) De Jongh, L. J.; Miedema, A. R. *Adv. Phys.* **1974**, *23*, 1.
- (15) Willett, R. D.; Place, H.; Middleton, M. *J. Am. Chem. Soc.* **1988**, *110*, 8639.
- (16) Long, G. S.; Wei, M.; Willett, R. D. *Inorg. Chem.* **1997**, *36*, 3102.
- (17) Sekine, T.; Okuno, T.; Awaga, K. *Inorg. Chem.* **1998**, *37*, 2129.
- (18) Levstik, A.; Filipic, C.; Blinc, R.; Arend, H.; Kind, R. *Solid State Commun.* **1976**, *20*, 127.
- (19) Kind, R.; Plesko, S.; Günter, P.; Roos, J.; Fousek, J. *Phys. Rev. B: Condens. Matter* **1981**, *23*, 5301.
- (20) Onoda-Yamamuro, N.; Matsuo, T.; Suga, H. *J. Phys. Chem. Solids* **1992**, *53*, 935.
- (21) Mitzi, D. B.; Dimitrakopoulos, C. D.; Kosbar, L. L. *Chem. Mater.* **2001**, *13*, 3728.
- (22) Xu, Z.; Mitzi, D. B.; Medeiros, D. R. *Inorg. Chem.* **2003**, *42*, 1400.
- (23) Xu, Z.; Mitzi, D. B.; Dimitrakopoulos, C. D.; Maxcy, K. R. *Inorg. Chem.* **2003**, *42*, 2031.
- (24) Mitzi, D. B.; Medeiros, D. R.; DeHaven, P. W. *Chem. Mater.* **2002**, *14*, 2839.
- (25) Mitzi, D. B.; Dimitrakopoulos, C. D.; Rosner, J.; Medeiros, D. R.; Xu, Z.; Noyan, C. *Adv. Mater.* **2002**, *14*, 1772.

Scheme 1



ies in this direction have revealed a solvent-free method of incorporating these hybrid materials into TFT (thin-film transistors) semiconductive channels through melt processing.<sup>25</sup>

In this paper, we seek to combine different organic cations within the same hybrid perovskite framework, so as to provide new opportunities to functionalize the organic components of the hybrid perovskites. Such effort was partly initiated by the observation that all reported crystal structures of such perovskites [e.g., (RNH<sub>3</sub>)<sub>2</sub>SnI<sub>4</sub>, R: organic groups] contain only one type of organic cation—in other words, no mixed-cation single-crystal structure has been previously determined (thin film samples that appeared to contain two different organic cations have been reported, although further study of the samples would be helpful for more complete characterization<sup>26</sup>). At the same time, an organic–inorganic perovskite containing two or more types of organic cations [e.g., (RNH<sub>3</sub>·R'NH<sub>3</sub>)SnI<sub>4</sub>, R, R': two different organic fragments] should provide further functional diversity and flexibility to the hybrid material.

The paper begins with the preparation and characterization of the hybrid perovskite containing in a 1:1 ratio the 2,3,4,5,6-pentafluorophenethylammonium and the 2-naphthyleneethylammonium cations (5FPEA·NEA)SnI<sub>4</sub>. The presence of the two cations within a single hybrid perovskite framework is verified by solution <sup>1</sup>H NMR, X-ray crystallographic studies (from both powder and single-crystal samples), and elemental analysis. We also present thin film optical absorption measurements of this compound. The paper then describes attempts to form hybrid perovskites containing the 5FPEA and NEA cations in ratios other than 1:1, demonstrating that such perovskite systems can be accessed through a rapid crystallization technique such as spin coating. Finally, a more complex mixed-cation system, which contains five rather different organic cations (Scheme 1), will be discussed. Here again, a single phase of the multication perovskite is achieved using the spin-coating method, as well as with a melt-quenching technique. The discovery of these multication systems points to a useful way to combine diverse organic functionalities within the perovskite framework through noncovalent mixing, as compared with the usually more strenuous multistep organic synthesis (for attaching organic functionalities onto a single molecule).

## Experimental Section

**Synthesis of 2-Naphthyleneethylamine.** The procedure is similar to that used for 2,3,4,5,6-pentafluorophenethylamine.<sup>27</sup> Under a flow of nitrogen gas, a lithium aluminum hydride (LiAlH<sub>4</sub>) solution in diethyl ether (1 M, 12 mL, 0.012

mol) was injected into a 100-mL flask equipped with a stir bar and capped by a septum. With vigorous stirring, a solution of aluminum chloride (anhydrous, 1.60 g, 0.012 mmol) in diethyl ether (anhydrous, 8.0 mL) was then rapidly injected through a cannula. After 3 min, a solution of 2-naphthylacetonitrile (2.0 g, 0.012 mol) in tetrahydrofuran (anhydrous, 16 mL) was injected into the above LiAlH<sub>4</sub>/AlCl<sub>3</sub> solution over a period of 3 min. Heat formation was hardly noticeable and a green/yellow solution was formed. After being stirred at room temperature for 3 h, the reaction mixture was chilled by an ice–water bath and icy water was dropwise and carefully added until no more bubbles formed. Sulfuric acid (6 N) was added to adjust the pH value to about 1. A saturated KOH solution was then added to make the mixture strongly basic (pH > 11). The mixture was then extracted by ether (3 × 30 mL) and the combined ether solution was dried over MgSO<sub>4</sub> and then evaporated to yield a yellow, viscous liquid as the raw product. The raw product was purified by vacuum distillation (bp 74 °C/60 mTorr, with the condenser slightly warmed to prevent solidification inside) to first yield a colorless liquid, which then quickly transformed at room temperature to give a white solid. <sup>1</sup>H NMR (400 MHz, acetone-*d*<sub>6</sub>): δ 7.87–7.82 (m, 3H), 7.74 (s, 1H), 7.50–7.42 (m, 3H), 3.56–3.52 (t, *J* = 7.4 Hz, 2H), 3.07–3.03 (t, *J* = 7.4 Hz, 2H), 2.90 (s, 2H). <sup>13</sup>C NMR (100 MHz, acetone-*d*<sub>6</sub>): δ 139.1, 134.2, 132.6, 128.2, 128.0, 127.9, 127.8, 127.3, 126.2, 125.5, 53.2, 37.7.

**Crystallization of (5FPEA·NEA)SnI<sub>4</sub>.** (5FPEA·NEA)SnI<sub>4</sub> crystals were grown by slowly evaporating an acetonitrile/anisole solution containing the organic and inorganic salts. First, 37.0 mg (0.10 mmol) of SnI<sub>2</sub> (Aldrich, anhydrous beads, 99.999%), 34 mg (0.10 mmol) of 2,3,4,5,6-pentafluorophenethylammonium iodide, and 30 mg (0.10 mmol) of 2-naphthyleneethylammonium iodide were added to a vial under an argon atmosphere. This mixture was then dissolved in 2.0 mL of anhydrous acetonitrile to form a yellow solution, which was then filtered through a Teflon filter (pore size: 0.2 μm). The filtrate was mixed with 2.0 mL of anhydrous anisole and placed in a loosely capped vial. Slow evaporation over a period of 3 days yielded platelike, bright red crystals (90 mg, yield 90%) suitable for X-ray single-crystal analysis. The powder X-ray diffraction pattern of the product showed a single phase, consistent with the single-crystal structure. Chemical analysis of the product (C<sub>20</sub>H<sub>21</sub>F<sub>5</sub>N<sub>2</sub>)SnI<sub>4</sub> yielded: Calcd [C (23.77%), H (2.09%), N (2.77%)]; found [C (23.60%), H (2.08%), N (2.78%)]. Solution <sup>1</sup>H NMR (400 MHz, CD<sub>3</sub>CN) indicated a 1:1 ratio of the 5FPEA and NEA cations: δ 7.94–7.89 (m, 3H), 7.82 (s, 1H), 7.56–7.53 (m, 2H), 7.47–7.44 (m, 1H), 6.60 (s, broad, 6H), 3.37–3.34 (t, *J* = 7.3 Hz, 2H), 3.24–3.16 (m, 6H). For comparison, <sup>1</sup>H NMR (400 MHz, CD<sub>3</sub>CN) for (5FPEA)<sub>2</sub>SnI<sub>4</sub>: 6.63 (s, broad, 3H), 3.25–3.20 (m, 2H), 3.17–3.13 (m, 2H). <sup>1</sup>H NMR (400 MHz, CD<sub>3</sub>CN) for (NEA)<sub>2</sub>SnI<sub>4</sub>: δ 7.94–7.89 (m, 3H), 7.82 (s, 1H), 7.57–7.51 (m, 2H), 7.47–7.43 (m, 1H), 6.46 (s, broad, 3H), 3.37–3.33 (t, *J* = 7.0 Hz, 2H), 3.22–3.18 (t, *J* = 7.2 Hz, 2H).

**X-ray Crystallography.** A blocklike crystal (0.3 × 0.2 × 0.03 mm) of (5FPEA·NEA)SnI<sub>4</sub> was selected under a microscope and attached to the end of a quartz fiber with 5 min epoxy. A full sphere of data was collected at room temperature on a Bruker SMART CCD diffractometer, equipped with a normal focus 2.4-kW sealed tube X-ray source (Mo Kα radiation). Intensity data were collected with a detector distance of approximately 5.0 cm, in 2272 frames with increasing ω. The increment in ω between each frame was 0.3°. An empirical absorption correction based on equivalent reflections was applied to the intensity data.<sup>28</sup>

The X-ray diffraction produced on the CCD frames sharp, well-defined spots as well as some streaks (indicating some disorder or unresolved superstructure), as has been seen in many other tin(II) iodide-based hybrid structures.<sup>21</sup> The current subcell was first indexed from the sharp reflections handpicked from the CCD frames and then refined in the

(26) Era, M.; Shimizu, A. *Mol. Cryst. Liq. Cryst.* **2001**, *371*, 199.

(27) Filler, R.; Chen, W.; Woods, S. M. *J. Fluorine Chem.* **1995**, *73*, 95.

(28) Sheldrick, G. M. *SADABS*; Institut für Anorganische Chemie der Universität Göttingen: Göttingen, Germany, 1997.

**Table 1. Crystallographic Data for (5FPEA·NEA)SnI<sub>4</sub>**

chemical formula	C <sub>20</sub> H <sub>21</sub> N <sub>2</sub> F <sub>5</sub> SnI <sub>4</sub>
formula weight	1010.68
space group	C2/c (No. 15)
<i>a</i> , Å	37.040(7)
<i>b</i> , Å	6.161(1)
<i>c</i> , Å	12.345(3)
$\beta$ , deg.	101.84(3)
<i>V</i> , Å <sup>3</sup>	2757(1)
<i>Z</i>	4
$\rho_{\text{calcd}}$ , g/cm <sup>3</sup>	2.435
wavelength (Å)	0.71073 (Mo K $\alpha$ )
absorption coefficient ( $\mu$ ), cm <sup>-1</sup>	54.51
R1 <sup>a</sup>	0.0653 ( <i>I</i> > 2 $\sigma$ ( <i>I</i> ))
wR2 <sup>b</sup>	0.1225 ( <i>I</i> > 2 $\sigma$ ( <i>I</i> ))

$$^a R1 = \sum(|F_o| - |F_c|)/\sum(|F_o|), ^b wR2 = \{\sum[w(F_o^2 - F_c^2)^2]/\sum[w(F_o^2)]\}^{1/2}.$$

**Table 2. Selected Bond Distances (Å) and Angles (deg) for (5FPEA·NEA)SnI<sub>4</sub>**

Sn–I(1)	3.184(1)	I(1)–Sn–I(2)	89.16(4)
Sn–I(1) <sup>a</sup>	3.184(1)	I(1) <sup>a</sup> –Sn–I(2)	90.09(4)
Sn–I(2) <sup>a</sup>	3.136(2)	I(2)–Sn–I(2) <sup>b</sup>	179.81(1)
Sn–I(2) <sup>b</sup>	3.181(2)	I(2) <sup>a</sup> –Sn–I(3) <sup>c</sup>	90.14(4)
Sn–I(3)	3.142(2)	I(2) <sup>b</sup> –Sn–I(3) <sup>d</sup>	89.67(4)
Sn–I(3) <sup>c</sup>	3.186(2)	I(2)–Sn–I(3)	90.41(4)
		I(3)–Sn–I(3) <sup>d</sup>	179.39(5)
I(1) <sup>a</sup> –Sn–I(1)	179.23(5)	I(3)–Sn–I(1) <sup>a</sup>	88.25(4)
I(1) <sup>a</sup> –Sn–I(2) <sup>b</sup>	89.92(4)	I(3)–Sn–I(1)	91.59(5)
I(1)–Sn–I(2) <sup>b</sup>	90.84(4)	I(3)–Sn–I(2) <sup>b</sup>	89.78(4)
I(1) <sup>a</sup> –Sn–I(3) <sup>c</sup>	88.69(4)	Sn <sup>c</sup> –I(3)–Sn	154.55(5)
I(1)–Sn–I(3) <sup>c</sup>	91.48(4)	Sn–I(2)–Sn <sup>e</sup>	154.48(5)

<sup>a</sup>  $-x, y, -z + 0.5$ . <sup>b</sup>  $-x, y - 1, -z + 0.5$ . <sup>c</sup>  $-x, -y, -z + 1$ . <sup>d</sup>  $x, -y, z - 0.5$ . <sup>e</sup>  $x, y + 1, z$ .

integration process. The structure was solved and refined with SHELXL 97. First, the Sn and I atoms were located by direct method. The N, F, and C atoms were then located using successive Fourier difference maps. All non-hydrogen atoms (Sn, I, C, N, and F) were refined anisotropically, while the hydrogen atoms were not located. The basal iodine atoms were refined as disordered over two symmetry-related sites, with an occupancy fixed at 0.5, whereas both the tin and apical iodine atoms are not disordered. Such crystallographic disordering in the inorganic sheet is commonly found in other layered perovskites.<sup>21,29</sup> The disordering of the organic components bears new features with respect to previously reported systems, as a result of the mixing of the organic cations and will be discussed in the Results and Discussion section. The occupancies of the carbon (from both cations) and fluorine (from 5FPEA) sites were all fixed at 0.5 since chemical synthesis and solution <sup>1</sup>H NMR spectra established a 1:1 ratio of the 5FPEA and NEA organic cations. The minimum and maximum peaks in the final difference Fourier maps corresponded to  $-0.807$  and  $0.795$  e/Å<sup>3</sup>. Selected crystallographic results are summarized in Table 1. Selected bond distances and angles are summarized in Table 2. A complete listing of crystallographic data, along with anisotropic displacement parameters, is given as Supporting Information.

**Film Deposition (Spin Coating).** Films of the perovskites were prepared in a nitrogen-filled drybox by spin coating a methanol solution on quartz substrates. The concentration for single-cation perovskites, such as (5FPEA)<sub>2</sub>SnI<sub>4</sub>, was equivalent to 20 mg of perovskite/1.6 mL of methanol and, for mixed-cation systems, a concentration of 20 mg/0.8 mL was used. The solutions of mixed-cation composites were made by dissolving the single-cation perovskites in various molar ratios [e.g., (5FPEA)<sub>2</sub>SnI<sub>4</sub>:(NEA)<sub>2</sub>SnI<sub>4</sub> = 2:1 and 1:2]. The substrate surface was first flooded by the solution and a spinning cycle was then initiated (1-s ramp to 3000 rpm; dwell 30 s at 3000 rpm). The substrate was then annealed at 70 °C for 15 min to remove

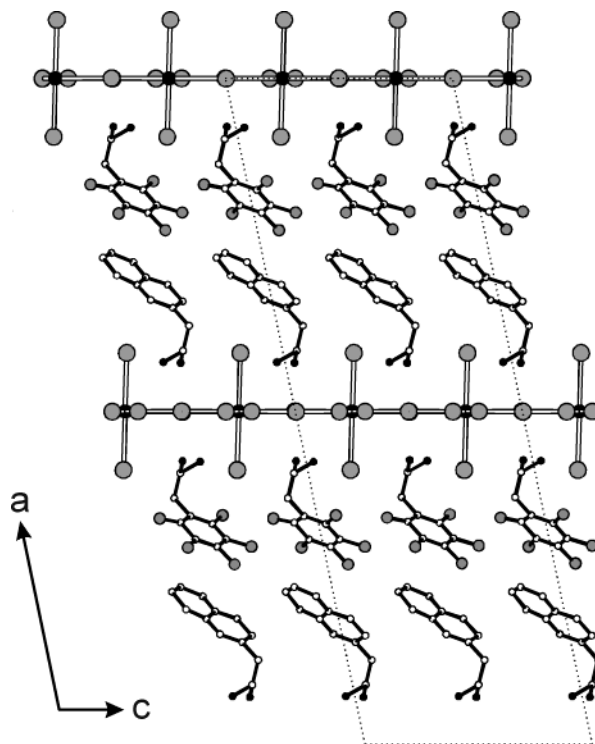


**Figure 1.** A structural model for the crystal of (5FPEA·NEA)SnI<sub>4</sub> viewed along the *b* axis. I, large gray sphere; Sn, large black sphere (partly eclipsed by I atoms); C, small open sphere; N, small black sphere; F, medium gray sphere. The disordering of the organic cations is omitted here. See text for the discussion on the disordering.

residual solvent and improve film quality. The films thus formed exhibited well-defined (*h* 0 0) X-ray diffraction peaks, indicating that the films were well-crystallized and highly oriented. For the five-cation system (see Scheme 1 for the five cations), the individual single-cation perovskites were first mixed and ground in equal amounts (by weight). The solution concentration was equivalent to 20 mg of perovskite mixture/0.8 mL of methanol and the subsequent steps were identical to those described above for the binary mixed-cation films.

**Film Deposition (Melt Processing for the Five-Cation System).** Under an inert atmosphere, the five single-cation perovskites were first mixed and ground in equal amounts (by weight). A temperature-controlled hot plate with an 8- $\mu$ m-thick Kapton sheet (ca. 3  $\times$  3 cm) was preheated to 220 °C. A small scoop of the perovskite mixture ( $\sim$  1 mg) was then placed onto the Kapton sheet. The melting of the perovskite mixture is almost instantaneous and a second Kapton sheet was immediately deposited to cover the melt. Capillary action spread the melt rather uniformly between the two Kapton sheets and the sandwiched molten film was allowed to stay on the hot plate for about 10 s. The melt was then removed from the hot plate and it at once solidified into a dark red film between the Kapton sheets.

**Optical Properties.** Absorption spectra were obtained at room temperature on spin-coated films (deposited on quartz disks) of the hybrid perovskites. The instrument is a Hewlett-Packard UV–vis 8543 spectrophotometer.

## Results and Discussion

**Crystal Structure of (5FPEA·NEA)SnI<sub>4</sub>.** The crystal structure of (5FPEA·NEA)SnI<sub>4</sub> was solved using a disordered model in the space group C2/c [*a* = 37.040(7) Å, *b* = 6.161(1) Å, *c* = 12.345(3) Å,  $\beta$  = 101.84(3)°, and *Z* = 4], with corner-sharing SnI<sub>6</sub> octahedral units forming the perovskite sheets alternating with layers of the organic cations (Figure 1). The current space

(29) Mitzi, D. B.; Medeiros, D. R.; Malenfant, P. R. L. *Inorg. Chem.* **2002**, *41*, 2134.

group and similar sets of unit cell parameters have been commonly found in other single-cation hybrid perovskite crystals such as (2-FPEA)<sub>2</sub>SnI<sub>4</sub> and (5FPEA)<sub>2</sub>SnI<sub>4</sub>·C<sub>6</sub>H<sub>6</sub>.<sup>21,29</sup> Bond distances and angles of the perovskite sheets are listed in Table 2, where the Sn–I bond lengths range from 3.14 to 3.19 Å and the two Sn–I–Sn angles are 154.6° and 154.5°. As can be seen, the bonding geometry around the Sn atom is close to being octahedral, indicating minimal chemical stereoactivity of the tin(II) 5s lone pair electrons. The bonding geometry and the Sn–I–Sn bond angle have been found to be related to the band gap and corresponding exciton energy of the semiconducting SnI<sub>4</sub><sup>2-</sup>-based perovskites.<sup>21–23</sup>

The presence of two individual organic cations in (5FPEA·NEA)SnI<sub>4</sub> causes new features of disordering to the structural solution with respect to the nominally isostructural single-cation systems<sup>21,29</sup> since the current diffraction data do not completely resolve the positions of the two cations. The ethylammonium side chain atoms and the carbon atoms on the aromatic ring from the 5FPEA cation are located on the same crystallographic positions as the corresponding atoms (the side chain and its neighboring benzoid ring) from the NEA cation. Physically reasonable intermolecular distances, however, provide some information about the local ordering with regard to the relative positions of the 5FPEA and NEA cations. For example, within the subcell model discussed here, unreasonable C···F and C···C contacts among the molecules (within and between organic cation layers) occur if the 5FPEA and NEA cations are placed next to each other within the same cation layer, that is, 2.6 Å C···F contacts (van der Waals distance: 3.17 Å<sup>30</sup>) within the single layer and 2.9 Å C···C distances (van der Waals distance: 3.40 Å<sup>30</sup>) between naphthylene moieties across the organic layers. The typical fluoroaryl–aryl interactions (as will be discussed more below) therefore seem to occur mainly across the two layers of organic cations confined between the neighboring perovskite sheets. One logical packing model for the organic cations, in which each of the two layers consists of the same type of organic cation, is shown in Figure 1. The streaks in the CCD frames, however, clearly point to a poorly ordered superstructure, which is not taken into account in the current model, and we therefore cannot completely discount the possibility of organic cation disorder (or mixing) within a given cation layer.

The 1:1 organic cation ratio of (5FPEA·NEA)SnI<sub>4</sub> is probably stabilized by the fluoroaryl–aryl interaction, which is commonly found to be a rather strong and directing interaction between arene and perfluorinated arene molecules.<sup>31–36</sup> The fluoroaryl–aryl interaction is imputed to arise from quadrupole–quadrupole interac-

tions and generally leads to face-to-face aromatic stacking within the molecular aggregates.<sup>37,38</sup> Previously, fluoroaryl–aryl interactions have been used to introduce guest molecules (e.g., C<sub>6</sub>H<sub>6</sub> and C<sub>6</sub>F<sub>6</sub>) within the van der Waals gap of the layered perovskites (5FPEA)<sub>2</sub>SnI<sub>4</sub> (5FPEA = 2,3,4,5,6-pentafluorophenethylammonium) and (PEA)<sub>2</sub>SnI<sub>4</sub> to produce the intercalation compounds (5FPEA)<sub>2</sub>SnI<sub>4</sub>·C<sub>6</sub>H<sub>6</sub> and (PEA)<sub>2</sub>SnI<sub>4</sub>·C<sub>6</sub>F<sub>6</sub>.<sup>29</sup> The local ordering deduced from the above crystallographic model (see also Figure 1) indicates that the fluoroaryl–aryl interaction between the 5FPEA layer and the NEA layer is typical, with each 5FPEA cation being approached by an NEA cation in an offset face-to-face or partially eclipsed manner (see Figure 1S in the Supporting Information), forming relatively short C···C distances of 3.36 Å and above and C···F distances of 3.41 Å and above. For comparison, in (5FPEA)<sub>2</sub>SnI<sub>4</sub>·C<sub>6</sub>H<sub>6</sub>, the shortest C···C contact between the benzene and pentafluorophenyl moieties is 3.49 Å and the shortest C···F contact 3.30 Å.<sup>29</sup>

**Beyond the 1:1 Organic Cation Ratio.** The 1:1 ratio compound (5FPEA·NEA)SnI<sub>4</sub> being achieved, we attempted to access hybrid systems containing the two organic cations in different ratios. Slow evaporation of a methanol solution containing (5FPEA)<sub>2</sub>SnI<sub>4</sub> and (NEA)<sub>2</sub>SnI<sub>4</sub> in 2:1 or 1:2 molar ratios yielded mixtures of the 1:1 ratio compound (5FPEA·NEA)SnI<sub>4</sub> and the remaining single-cation compound [i.e., (5FPEA)<sub>2</sub>SnI<sub>4</sub> or (NEA)<sub>2</sub>SnI<sub>4</sub>]. Such results seem to suggest that the 1:1 ratio compound is thermodynamically favored, perhaps due to the potential for fluoroaryl–aryl interaction between neighboring layers.

Further experiments revealed, however, that compounds containing the two organic cations beyond the 1:1 ratio can be accessed by spin coating from organic solutions as a very rapid deposition/crystallization process. In particular, we have tested methanol solutions containing (5FPEA)<sub>2</sub>SnI<sub>4</sub> and (NEA)<sub>2</sub>SnI<sub>4</sub> in 2:1 and 1:2 ratios. The X-ray powder diffraction patterns for the thin films thus formed are shown in Figure 2. For comparison, X-ray diffraction patterns for similarly prepared films of (5FPEA·NEA)SnI<sub>4</sub> and the two single-cation compounds (5FPEA)<sub>2</sub>SnI<sub>4</sub> and (NEA)<sub>2</sub>SnI<sub>4</sub> are also included. As is typical of similar layered perovskites, all the powder patterns show a distinct (*h*, 0, 0) series of reflections, indicating the highly preferred *a* axis orientation of the crystallites, which is due to the strong two-dimensional character of these crystal structures. The single-phase nature of either the 2:1 or 1:2 system is evident from the powder pattern, indicating that the two cations are now uniformly integrated within a single hybrid perovskite framework. The powder patterns also indicate a monotonic widening of the spacing between the inorganic layers among these five systems from (5FPEA)<sub>2</sub>SnI<sub>4</sub> to (NEA)<sub>2</sub>SnI<sub>4</sub>. No diffraction peak broadening for the 2:1 and 1:2 mixed cation samples (relative to the other samples in Figure 2) is observed, indicating that organic cation mixing does not reduce the crystallinity of spin-coated films. We surmise that the inorganic framework forms faster than the segregation of the organic cations, and therefore, in rapid deposition, it manages to trap the mixed organic

(30) Bondi, A. J. *Phys. Chem.* **1964**, *68*, 441.

(31) Patrick, C. R.; Prosser, G. S. *Nature* **1960**, *187*, 1021.

(32) Coates, G. W.; Dunn, A. R.; Henling, L. M.; Dougherty, D. A.; Grubbs, R. H. *Angew. Chem., Int. Ed. Engl.* **1997**, *36*, 248.

(33) Coates, G. W.; Dunn, A. R.; Henling, L. M.; Ziller, J. W.; Lobkovsky, E. B.; Grubbs, R. H. *J. Am. Chem. Soc.* **1998**, *120*, 3641.

(34) Dai, C.; Nguyen, P.; Marder, T. B.; Scott, A. J.; Clegg, W.; Viney, C. *Chem. Commun.* **1999**, 2493.

(35) Ponzini, F.; Zagha, R.; Hardcastle, K.; Siegel, J. S. *Angew. Chem., Int. Ed.* **2000**, *39*, 2323.

(36) Feast, W. J.; Lövenich, P. W.; Puschmann, H.; Taliani, C. *Chem. Commun.* **2001**, 505.

(37) Brown, N. M. D.; Swinton, F. L. *Chem. Commun.* **1974**, 770.

(38) Williams, J. H. *Acc. Chem. Res.* **1993**, *26*, 593.

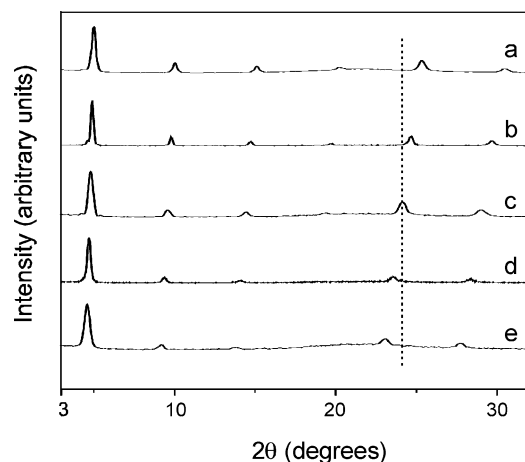


**Figure 2.** Room-temperature X-ray diffraction patterns (Cu K $\alpha$ ,  $\lambda = 1.5418$  Å) for the spin-coated thin films of the hybrid perovskite series comprised of various (5FPEA) $_2$ SnI $_4$ :(NEA) $_2$ SnI $_4$  ratios: (a) 1:0 [i.e., (5FPEA) $_2$ SnI $_4$ ]; (b) 2:1; (c) 1:1 [i.e., (5FPEA·NEA)SnI $_4$ ]; (d) 1:2; (e) 0:1 [i.e., (NEA) $_2$ SnI $_4$ ]. The dashed line highlights the evolution of the  $2\theta$  values for the (10, 0, 0) peaks: (a) 25.40°; (b) 24.74°; (c) 24.22°; (d) 23.61°; (e) 23.14°.

cations into something like a solid solution. Note that for the monocationic compounds (5FPEA) $_2$ SnI $_4$  and (NEA) $_2$ SnI $_4$  and the 1:1 compound (5FPEA·NEA)SnI $_4$ , the  $a$  axis parameter derived from the diffraction pattern of the spin-coated films agrees with that of the bulk sample.

**Optical Properties.** Optical absorption spectra of semiconducting hybrid perovskites based on SnI $_4^{2-}$  sheets exhibit strong room-temperature exciton peaks associated with the electronic band gaps.<sup>9,10,39,40</sup> Previous work has shown that such exciton peaks can be effectively shifted by varying the dielectric constant of the organic layer<sup>39</sup> and by chemical modification of the organic cations (which usually induces significant changes in the bonding features of the inorganic sheets).<sup>21–23</sup> The above mixed-cation systems provide for a more versatile method of tuning the electronic properties of the hybrid materials since one can in principle vary the ratio of the two cations in a continuous manner and thereby fine-tune their influence on the electronic structures. Like above, here we have chosen three ratios of the (5FPEA) $_2$ SnI $_4$  and (NEA) $_2$ SnI $_4$  compounds (2:1, 1:1, 1:2) to spin-coat thin films for optical property studies. For comparison we will also present results on the two single-cation end members.

As shown in Figure 3, all the five systems exhibit single, well-defined exciton peaks associated with the band gap, consistent with their phase purity indicated by the X-ray powder patterns (Figure 2). The (5FPEA) $_2$ SnI $_4$ :(NEA) $_2$ SnI $_4$  ratios of the systems and their respective exciton wavelengths are as follows: (a) 1:0 [i.e., (5FPEA) $_2$ SnI $_4$ ], 572 nm; (b) 2:1, 579 nm; (c) 1:1 [i.e., (5FPEA·NEA)SnI $_4$ ], 588 nm; (d) 1:2, 595 nm; (e) 0:1 [i.e., (NEA) $_2$ SnI $_4$ ], 602 nm. Thus, the exciton peak consistently shifts to longer wavelengths as the proportion of the NEA cation is increased. Meanwhile, as is seen in Figure 3, the band

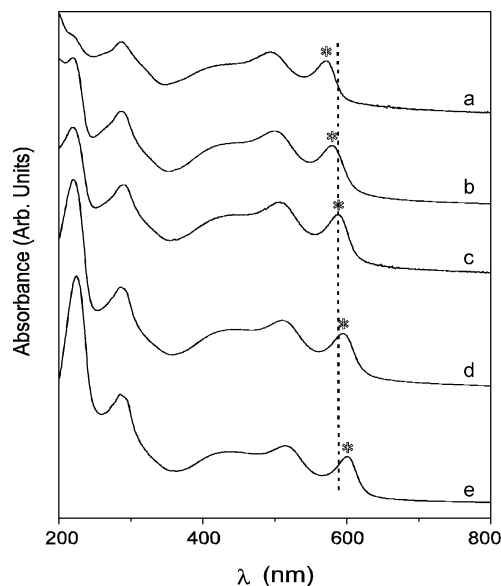


**Figure 3.** Room-temperature UV-vis absorption spectra for the spin-coated thin films of the hybrid perovskite series comprised of various (5FPEA) $_2$ SnI $_4$ :(NEA) $_2$ SnI $_4$  ratios: (a) 1:0 [i.e., (5FPEA) $_2$ SnI $_4$ ]; (b) 2:1; (c) 1:1 [i.e., (5FPEA·NEA)SnI $_4$ ]; (d) 1:2; (e) 0:1 [i.e., (NEA) $_2$ SnI $_4$ ]. The exciton peaks are marked by asterisks. The dashed line clarifies the shifts in the peak positions.

edges of the series exhibit similar evolution as the ratio of the two cations is changed. The naphthylene group as a chromophore shows its characteristic absorption peak around 220 nm. As is seen from Figure 3a–e, this peak grows ever more intense relative to the exciton peak, in keeping with the concentration of the naphthylene component in the system.

**More Complex Multication Systems.** From the diverse ratios of the two cations incorporated in the above binary perovskite composites, we suspect that spin coating may be more generally effective in integrating different organic cations within a uniform perovskite framework. To test this idea, we have chosen to study a more complex system containing in equal amounts five different (RNH $_3^+$ ) $_2$ SnI $_4$ -type perovskites (the five RNH $_3^+$  ions are listed in Scheme 1). The five RNH $_3^+$  ions thus chosen encompass rather diverse functionalities and structures and should provide cogent proof for the versatility of the mixed-cation approach, if a single perovskite phase is to be formed from this combination.

First, we conducted a regular crystallization experiment: a methanol solution containing the five single-cation perovskites was evaporated over a period of about 30 min by flowing nitrogen gas over the solution. The resultant solid sample turned out to be a rather complicated mixture comprising several different perovskite phases, as is indicated by its powder pattern in Figure 4a. The analysis of such a mixture is beyond the scope of this paper because the ultimate goal here is to incorporate all these cations within a single perovskite phase.

Let us now turn to the results of the spin-coating experiment, which indeed yielded a single-phase product. The X-ray powder pattern of the spin-coated thin film from a methanol solution is shown in Figure 4b, which indicates a single perovskite phase, with a spacing between the perovskite layers (17.7 Å) close to that of the average (17.6 Å) of those of the constituent phases.

(39) Hong, X.; Ishihara, T.; Nurmikko, A. V. *Phys. Rev. B: Condens. Matter* **1992**, *45*, 6961.

(40) Ishihara, T. In *Optical Properties of Low-Dimensional Materials*; Ogawa, T., Kanemitsu, Y., Eds.; World Scientific: Singapore, 1995; pp 288–339.

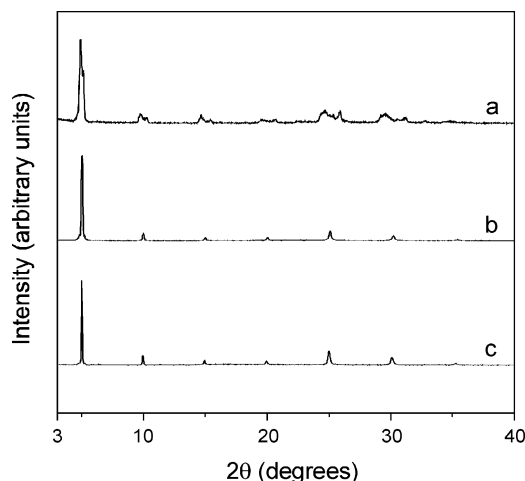


**Figure 4.** Room-temperature X-ray diffraction patterns (Cu K $\alpha$ ,  $\lambda = 1.5418$  Å) for the tin(II) iodide perovskite products from interacting five single-cation perovskites (RNH<sub>3</sub>)<sub>2</sub>SnI<sub>4</sub> (the five R groups are listed in Scheme 1): (a) by slow evaporation from a methanol solution; (b) by spin coating from a methanol solution; (c) by rapid cooling of the molten mixture.

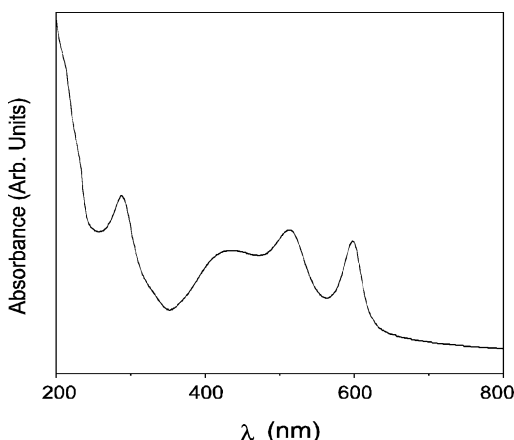


**Figure 5.** Room-temperature UV-vis absorption spectra for a thin film of the multication hybrid perovskite made by spin-coating from a methanol solution containing five single-cation perovskites (RNH<sub>3</sub>)<sub>2</sub>SnI<sub>4</sub> (the five R groups are listed in Scheme 1). This thin film sample corresponds to that of Figure 4b.

In addition, no peak broadening is observed in the current diffraction pattern as compared with those of the above two-cation systems (Figure 2), indicating that the phase purity and crystallinity of the solid product are not affected by the increased number of different organic cations. The optical absorption spectrum of the spin-coated film is shown in Figure 5. The single, well-defined exciton peak (at 598 nm) is also typical of a single-phase perovskite based on the SnI<sub>4</sub><sup>2-</sup> layer.

To further demonstrate the inclusion of all five organic cations in the current system, we carried out a melt processing of the mixture made from the five constituent single-cation perovskites. For this, a mixture of the five individual perovskites was melted at 220 °C and then rapidly cooled to room temperature to produce a homogeneous multication system. The X-ray powder pattern of this melt-processed sample is shown in Figure 4c, which indicates a single perovskite phase, with an interlayer spacing (17.8 Å) similar to both that of the above spin-coated sample (17.7 Å) and the average (17.6 Å) of those of the constituent phases. In addition, the peak

shapes are practically the same for both the spin-coated and melt-processed samples, indicating a similar level of phase homogeneity in the solid products. Finally, solution (in CD<sub>3</sub>OD) <sup>1</sup>H NMR spectra for the mixture before and after melting are identical, indicating that no chemical decomposition occurred for the organic cations in the course of melting. Taken together, these experiments render further evidence for the making of a single-phase hybrid perovskite containing the five original organic cations.

## Conclusions

This paper describes our effort to make multifunctional hybrid perovskites by incorporating different organic cations within the SnI<sub>4</sub><sup>2-</sup>-based perovskite framework. For attractive cation pairs, such as the 5FPEA·NEA pair, a clear-cut 1:1 ratio hybrid perovskite can be obtained in both rapid (i.e., spin coating) and slow crystallization processes—this ratio therefore seems to produce a thermodynamically controlled product. For ratios other than 1:1 or for multication systems where attractive interactions among the organic cations are less distinct, one generally may still achieve a single-phase perovskite through spin coating or melt quenching (given an appropriately compatible choice of organic cations). Such multication perovskites appear to be kinetic products whose formation is favored by a very rapid crystallization process and can be regarded as a certain type of solid solution.

The making of multifunctional organic materials is usually dependent upon multistep organic synthesis for attaching the various functional groups onto a specific molecular substrate. Through synthesizing and characterizing various mixed-cation perovskites, we have demonstrated a simple method of making multifunctional organic materials in the context of hybrid perovskites. Besides the easy implementation (i.e., physical mixing), the current method offers a unique advantage in that it allows organic cations to be combined in various ratios within a single perovskite phase. Such structural flexibility should prove particularly useful for fine-tuning the electronic structures of the inorganic frameworks of the SnI<sub>4</sub><sup>2-</sup>- or PbI<sub>4</sub><sup>2-</sup>-based perovskites as semiconductive or luminescent materials.<sup>41,42</sup> In addition, this method also allows combining of organic functional groups to optimize the interface interactions in thin-film transistors (TFTs) and other devices. For example, by incorporating a thiol-containing cation and a hydroxyl-containing cation into the perovskite framework, one can hope to optimize the interaction of the semiconductive channel with metal (e.g., Au) electrodes, as well as the SiO<sub>2</sub> dielectric layer.

**Supporting Information Available:** Full crystallographic data for (5FPEA·NEA)SnI<sub>4</sub> (CIF). A figure showing the face-to-face interaction between the 2,3,4,5,6-pentafluorophenethylammonium (5FPEA) and 2-naphthylethylammonium (NEA) cations in the crystal structure of (5FPEA·NEA)SnI<sub>4</sub> (PDF). This material is available free of charge via the Internet at <http://pubs.acs.org>.

CM034267J

(41) Gebauer, T.; Schmid, G. *Z. Anorg. Allg. Chem.* **1999**, 625, 1124.  
(42) Chondroudis, K.; Mitzi, D. B. *Chem. Mater.* **1999**, 11, 3028.